

Available online at www.sciencedirect.com

ScienceDirect

journal homepage: <http://www.journals.elsevier.com/nuclear-engineering-and-technology/>

Original Article

HAZARD ANALYSIS OF TYPHOON-RELATED EXTERNAL EVENTS USING EXTREME VALUE THEORY

YOCHAN KIM ^{a,*}, SEUNG-CHEOL JANG ^a, and TAE-JIN LIM ^b^a Integrated Safety Assessment Division, Korea Atomic Energy Research Institute (KAERI), 1045 Daedeokdaero, Yuseong-gu, Daejeon 305-353, Republic of Korea^b Department of Industrial Information Systems Engineering, Soongsil University, Seoul 156-743, Republic of Korea

ARTICLE INFO

Article history:

Received 2 April 2014

Received in revised form

22 August 2014

Accepted 25 August 2014

Available online 21 January 2015

Keywords:

External event

Extreme value theory

Hazard analysis

Natural event

Return level

Return period

ABSTRACT

Background: After the Fukushima accident, the importance of hazard analysis for extreme external events was raised.**Methods:** To analyze typhoon-induced hazards, which are one of the significant disasters of East Asian countries, a statistical analysis using the extreme value theory, which is a method for estimating the annual exceedance frequency of a rare event, was conducted for an estimation of the occurrence intervals or hazard levels. For the four meteorological variables, maximum wind speed, instantaneous wind speed, hourly precipitation, and daily precipitation, the parameters of the predictive extreme value theory models were estimated.**Results:** The 100-year return levels for each variable were predicted using the developed models and compared with previously reported values. It was also found that there exist significant long-term climate changes of wind speed and precipitation.**Conclusion:** A fragility analysis should be conducted to ensure the safety levels of a nuclear power plant for high levels of wind speed and precipitation, which exceed the results of a previous analysis.

Copyright © 2015, Published by Elsevier Korea LLC on behalf of Korean Nuclear Society.

1. Introduction

After the Fukushima accident, the importance of hazard analysis for extreme external events has been recognized for the safety of nuclear power plants [1,2]. Some external events can result in common cause failures or common cause initiators by simultaneously affecting diverse and redundant

safety systems [3,4]. Several articles have also indicated that external events are one of the primary sources inducing multiunit site risks [1–7]. Moreover, external events can have a crucial influence on the physical environment in instrument and control systems as well as increase the stress of the operators; hence, an external event can affect the reliability of operators who cope with the event [3,4,7].

* Corresponding author.

E-mail address: yochankim@kaeri.re.kr (Y. Kim).

This is an Open Access article distributed under the terms of the Creative Commons Attribution Non-Commercial License (<http://creativecommons.org/licenses/by-nc/3.0>) which permits unrestricted non-commercial use, distribution, and reproduction in any medium, provided the original work is properly cited.
<http://dx.doi.org/10.1016/j.net.2014.08.001>

1738-5733/Copyright © 2015, Published by Elsevier Korea LLC on behalf of Korean Nuclear Society.

To analyze the hazards of external events, it is possible to statistically estimate an extreme value if sufficient data exist. However, a statistical estimation based on an empirical distribution function does not yield useful information if we are interested in the probability of events that have a level beyond the range of observation [8].

The extreme value theory (EVT) provides asymptotic models to describe the distribution of a rare event and is a useful technique to analyze the annual frequency of exceedance [9]. EVT has been applied to a variety of fields such as natural hazards, finance risks, and the reliability of components or systems. Nonstationary models based on EVT have also been used to investigate long-term climate change, in particular global warming effects [10]. For these reasons, some nuclear safety reports have recommended EVT to evaluate various natural hazards of plant sites with important considerations for the evaluation process [3,11,12].

In this study, we evaluated typhoon-induced hazards, which are one of the significant disasters of East Asian countries using EVT. The data for four variables, i.e., maximum wind speed, maximum instant wind speed, hourly precipitation, and daily precipitation, have been collected by the Korean meteorological administration for 109 years. The parameters of EVT models for the variables were estimated, and 100-year return levels were predicted. The predicted results were also compared with previous research results or design limits of the nuclear power plant in the domestic site.

2. Materials and methods

2.1. EVT

Generally, there are two practical approaches of EVT: block maxima (BM) and peaks over threshold (POT) [13].

2.2. BM method

The BM method uses the maxima or minima within blocks of equal length such as the annual maxima of daily recorded wind speeds. Annual maxima/minima data are often used for satisfying robustness as well as the statistical power of analysis [9]. For the BM method, the generalized extreme value (GEV) distribution function is employed to describe the maxima if the blocks are large. The GEV distribution is expressed by:

$$G(z) = \exp\left\{-\left[1 + \xi \frac{z - \mu}{\sigma}\right]^{-1/\xi}\right\}, \quad (1)$$

Defined on the set $\{z : 1 + \xi(z - \mu)/\sigma > 0\}$, where $\mu \in \mathbb{R}$, $\sigma > 0$, and $\xi \in \mathbb{R}$ are the location, scale, and shape parameters respectively. Actually, the GEV comprises three different distributions: Weibull, Gumbel, and Frechet. When $\xi \rightarrow 0$, the GEV function corresponds to the Gumbel distribution, when $\xi > 0$, it arrives at the Frechet distribution, and when $\xi < 0$, it is reduced to a Weibull distribution. If z_p is the return level, which can be defined as the level that “is expected to be exceeded on average every $1/p$ years”, z_p is estimated by the following equation [9]:

$$z_p = \begin{cases} \mu - \frac{\sigma}{\xi} [1 - \{-\log(1-p)\}^{-\xi}], & \text{for } \xi \neq 0, \\ \mu - \sigma \log\{-\log(1-p)\}, & \text{for } \xi = 0, \end{cases} \quad (2)$$

where $G(z_p) = 1 - p$. In this equation, $T = 1/p$ is called the return period.

2.3. POT method

The POT method deals with observations that exceed a selected threshold rather than the annual maxima/minima of the raw data. Hence, the POT method can provide a way to meaningfully use a larger amount of data if the threshold is sufficiently low. The generalized Pareto (GP) distribution H for y exceeding a sufficiently large threshold u is used for the POT approach [9].

$$H(y) = 1 - \left(1 + \frac{\xi y}{\hat{\sigma}}\right)^{-\frac{1}{\xi}}, \quad (3)$$

defined for $\{y : y > 0 \text{ and } (1 + \frac{\xi y}{\hat{\sigma}}) > 0\}$, where $\hat{\sigma} = \sigma + \xi(u - \mu)$.

Similar to GEV, the GP distribution can be expressed by three extreme distributions according to the shape parameter ξ . In the case of $\xi > 0$, the GP distribution is equivalent to the usual Pareto distribution. For $\xi \rightarrow 0$, we obtain the exponential distribution. In addition, when $\xi < 0$, it becomes a beta distribution having a finite upper endpoint at $-\sigma/\xi$. According to Equation 3, the N -year return level z_N estimated by the GP distribution is produced by:

$$z_N = u + \frac{\hat{\sigma}}{\xi} \left[(Nn_y \zeta_u)^\xi - 1 \right]. \quad (4)$$

Here, ζ_u is the probability that an observation x exceeds the threshold u and n_y is the number of observations per year.

2.4. Previous analysis of Korean site

The preliminary safety analysis report of Shinkori Units 3 and 4 addressed safety standards of wind speed and rainfall considering the construction and management of nuclear power plants at the Korean site, Kori [14]. According to the report, the designed wind speed of Shinkori Units 3 and 4 was 45 m/s, and the maximum value of instantaneous wind speed records at the nearest cities was 43 m/s. In this report, the annual maximum instantaneous wind speed was also estimated using a Gumbel distribution. As a result, the biggest 100-year return level among the nearest cities was 42.6 m/s. By contrast, this report predicted the maximum possible amount of rainfall considering floods from the nearest river as 208 mm/h and 790 mm/d.

The results of the previous analysis can be improved through several considerations. First, it is possible to apply both the BM and POT methods and select a model that best describes the observations from the results of these methods. The EVT approaches, including GEV and GP distributions, can also allow fitting parameters under an assumption of more various distributions. Second, the temporal trends of meteorological variables can be considered during the return level prediction. Finally, data observed in the entire Korean territory can be used to understand nationwide effects of typhoons

Table 1 – Descriptive statistics of Korean typhoon data.

Variable	Maximum wind speed (m/s)	Maximum instantaneous wind speed (m/s)	Maximum hourly precipitation (mm/h)	Maximum daily precipitation (mm/d)
Observation	333	208	231	330
Missing observation	0	125	102	3
Measured year	109	71	75	109
Mean	20.432	28.173	30.97	122.95
Standard deviation	8.221	10.089	23.13	100.47
Median	19.6	27.55	24.8	106.35
Minimum	0	0	0	0
Maximum	51.8	60	100.5	870.5

or obtain more conservative results. This paper provides empirical results including these considerations.

2.5. Data

In this study, hazards related to typhoons were investigated because there are meteorological records related to Korean-specific typhoons for > 100 years, and thus there are sufficient data for a statistical analysis. Moreover, typhoons are recognized as one of the natural hazards that can cause a huge loss of life and property, and many other East Asian countries have experienced significant damage caused by typhoons [15,16]. According to the Nuclear Energy Agency report, some typhoons have also affected the safety of domestic nuclear power plants [3].

Four data variables on the wind speed and rainfall for each typhoon were investigated. (1) Maximum wind speed (m/s): maximum wind speed among the average velocities for every 10 minutes during a typhoon. (2) Maximum instantaneous wind speed (m/s): maximum wind speed during a typhoon. (3) Maximum hourly precipitation (mm): maximum hourly rainfall when under the influence of a typhoon. (4) Maximum daily precipitation (mm): maximum daily rainfall when under the influence of a typhoon.

The observations describe the wind speed and rainfall of 328 typhoons recorded for 109 years, from 1904 to 2012. The typhoons in 1920, 1947, 1988, 2001, and 2009 did not significantly affect the Korean Peninsula; hence, we assumed that there was neither rainfall nor wind during those 5 years, even though records exist of wind speeds and precipitation that are not related with typhoons. In addition, the maximum hourly precipitation has been recorded from 1937, and the maximum instantaneous wind speed has been recorded from 1940. Table 1 shows the basic descriptive statistics of the observations. It is notable that these observations are the maximum data of the entire Korean territory instead of any local area, while the data of a local area were used in the preliminary safety analysis report of Shinkori Units 3 and 4. The predicted levels in this study are expected to be larger than the data in the preliminary report.

2.6. Parameter estimation and model selection

In this study, the statistical models for the four variables were developed using both POT and BM approaches, and the final

models that better describe the observed values were selected based on the diagnostic plots. For the BM approach, the annual maxima of observations were used in the parameter estimation and return level prediction, while the POT approach used raw data for the target variables.

For an estimation of the parameters of a model produced by the POT or BM approach, different estimation methods can be used: graphical techniques, moment-based estimators, probability-weighted moments, and likelihood-based techniques [9]. However, many studies were conducted based on likelihood-based techniques, especially maximum likelihood estimation [13]. In this study, the location, scale, and shape parameters of the GEV and GP distributions were also estimated through a maximum likelihood estimation.

Although the POT approach has an advantage in that it allows more observations to estimate the parameters by adjusting threshold u , it is also difficult to determine the optimum threshold [9,13]. If the threshold is too low, the asymptotic basis of the model may be violated and biased. If the threshold is too high, few observations will be used for a parameter estimation and will produce a high variance. In this study, the thresholds were determined by two graphical methods, the mean residual life plot and parameter stability plot. The mean residual life plot is generated by the locus of points:

$$\left\{ u, \frac{1}{n_u} \sum_{i=1}^{n_u} (x_{(i)} - u) : u < x_{\max} \right\}, \quad (5)$$

where $x_{(i)}$ are observations that exceed u , and x_{\max} is the largest of $x_{(i)}$. The optimum threshold is selected where the mean residual plot is approximately linear. The parameter stability plot fits the GP distribution across a range of thresholds to check the stability of the parameter estimates. The optimum threshold is selected where the estimates in the parameter stability plot remain nearly constant.

For assessing the accuracy of the GEV and GP models fitted to the Korean typhoon data, the quantile–quantile (QQ) plot, probability–probability (PP) plot, return level plot, and density estimate plot were employed [9,13]. For an ordered sequence of observations $x_{(i)}$, the QQ plot and PP plot consist of the points in (6) and (7), respectively.

$$\left\{ \left[\hat{F}^{-1} \left(\frac{i}{n+1} \right), x_{(i)} \right] : i = 1, \dots, n \right\}, \quad (6)$$

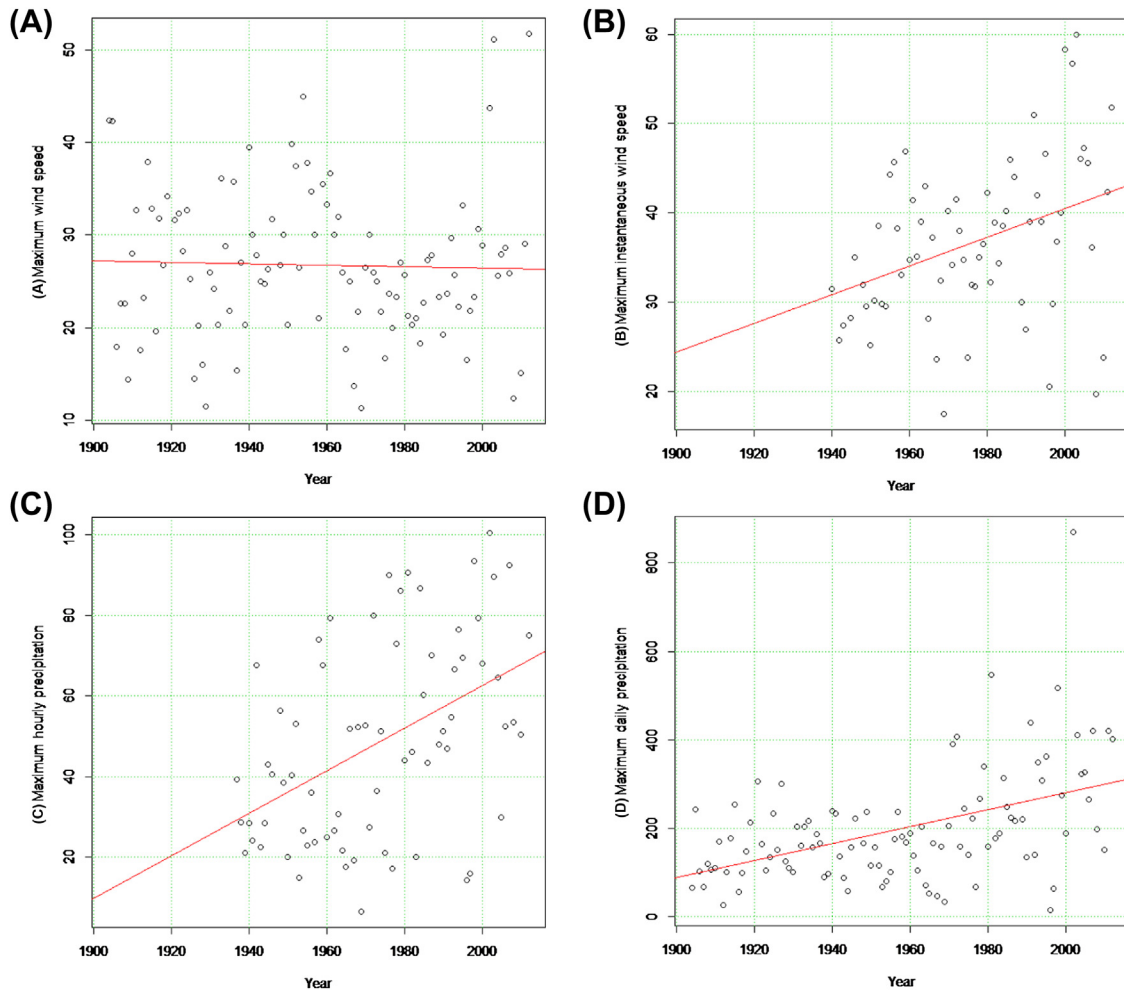


Fig. 1 – Scatter plots of annual maximum data. (A) Maximum wind speed, (B) maximum instantaneous wind speed, (C) maximum hourly precipitation, and (D) maximum daily precipitation.

$$\left\{ \left[\hat{F}\left(x_{(i)}\right), \frac{i}{n+1} \right] : i = 1, \dots, n \right\}, \quad (7)$$

where \hat{F} is the estimated distribution function. If the points in the QQ plot and PP plot approximately lie on the unit diagonal line, it is concluded that the generated model or function provides a plausible fit to the observations. Both plots deliver similar information; however, \hat{F} can be seen as reasonable only when all the scatter points in both plots are close to the reference lines because the two plots have different scales [9]. The return level plot shows the expected return levels for each return period. If the model-based curve and empirical estimates are in reasonable agreement, it can be declared that the generated model is suitable for the observations. The density estimate plot compares a histogram of the observations with a fitted density function.

To identify the effects of long-term climate change, nonstationary models that include time-dependent variables were also generated. For example, the location parameter, μ , of the GEV(μ, σ, ξ) distribution can be replaced by $\mu(t) = \beta_0 + \beta_1 t$ for a nonstationary model. In this study, variations through time in the observations are modeled by linear functions of location, scale, or shape parameters of the extreme value

models. The goodness-of-fit of the nonstationary models were validated by QQ plots and PP plots, and the new models were compared with stationary models through likelihood ratio tests. When the p -value of the likelihood ratio test was $< 5\%$ significance level, the nonstationary model was chosen.

The analyses in this paper were performed with the R statistical package `extRemes`, which is freely available from cran.r-project.org.

3. Results

Fig. 1 shows the scatter plots of the observed variables. Using the method explained above, the final distributions were determined, and the parameters estimated for each variable. As a result, the GP distributions were selected for all variables. This is because GP distributions are generally immune to 0 values, including 0s by the years in which no typhoon was observed, and can reflect more observations than GEV distributions. For the maximum instantaneous wind speed and two precipitation variables, temporal trends were observed; hence, the parameters were estimated by the linear functions of time (year). From the obtained model, the

Table 2 – Parameter estimates, standard errors, and 100-year return levels of the EVT models fitted to the four typhoon-related variables.

Variable	Selected distribution	Parameter estimates	Standard errors	100-year return level
Maximum wind speed	GP ($u = 20$)	<ul style="list-style-type: none"> Scale: 8.428 Shape: -0.167 	<ul style="list-style-type: none"> Scale: 0.869 Shape: 0.066 	48.424
Maximum instantaneous wind speed	GP ($u = 25$)	<ul style="list-style-type: none"> Scale: $0.059 y - 103.809$ Shape: $0.004 y - 8.681$ 	<ul style="list-style-type: none"> Scale_y: 0.000 Scale: 1.397 Shape_y: 0.000 Shape: 0.087 	<ul style="list-style-type: none"> stationary model: 58.415 nonstationary model from 2034: 82.424
Maximum hourly rainfall	GP ($u = 10$)	<ul style="list-style-type: none"> Scale: $0.099 y - 161.348$ Shape: $0.004 y - 8.118$ 	<ul style="list-style-type: none"> Scale_y: 0.002 Scale: 5.766 Shape_y: 0.000 Shape: 0.088 	<ul style="list-style-type: none"> stationary model: 103.161 non-stationary model from 2034: 180.862
Maximum daily rainfall	GP ($u = 100$)	<ul style="list-style-type: none"> Scale: $0.750 y - 1393.186$ Shape: 0.038 	<ul style="list-style-type: none"> Scale_y: 0.183 Scale: 355.294 Shape: 0.082 	<ul style="list-style-type: none"> stationary model: 655.628 nonstationary model from 2034: 848.387

100-year return levels of each variable were also predicted. For the three variables that were estimated by nonstationary models, the return levels by the stationary and nonstationary models were calculated to compare the effects of temporal trends. Because the value of the year should be inputted to calculate the return levels of the time-dependent models, we assumed the basis year as 2034, which is 20 years from now. Table 2 shows the parameter estimates, standard errors, and 100-year return levels of the EVT models, and Fig. 2 also shows diagnostic plots for each variable. The black lines on the return level plot for the maximum wind speed variable represent the return levels calculated for the return periods, and the blue lines show 95% confidence intervals of the return levels. The unbroken line on the density estimate plot shows the fitted density function for the maximum wind speed. By contrast, the PP plots and QQ plots for the nonstationary processes are depicted as diagnostic diagrams for the other variables.

4. Discussion

4.1. EVT method for external hazard analysis

In this paper, we propose a statistical method using EVT to analyze hazards of external events. The developed models describe the observed data well and extrapolate the return levels or exceedance probability of rare events. For example, the 100-year return levels in Table 2 and the return level plot in Fig. 2 reveal the predicted values about the return levels for a specific return period or probability. Moreover, it was found that there were significant time effects on the three variables (p -values of the likelihood tests: instantaneous wind speed = 0.002, hourly precipitation = 0.016, and daily precipitation < 0.001). The time-dependent models allowed us to forecast the amount of hazard considering the effects of long-term climate change. Compared with the previous stationary study, it is expected that the nonstationary models give more accurate results for natural hazards. When comparing the differences between return levels predicted by the stationary models and nonstationary models, it can be concluded that the hazards of Korean typhoons are enlarged by the effects of climate change.

When investigating natural hazards related to nuclear facilities by the EVT method, it is useful to review the guidelines of the International Atomic Energy Agency and Atomic Energy Licensing Board, as well as general manuals of EVT analysis [11,12]. The examples of the analysis guidelines from the reports can be summarized as follows: (1) when identifying, analyzing, and characterizing a hazard, there exist procedural uncertainty and subjective interpretation of the analyzers; hence, consistent analysis and interpretation procedures should be applied; (2) the gaps, trends, jumps, missing values, and outliers in the available data should be dealt with appropriately; (3) the target area and type and scope of information to be investigated should be determined according to the characteristics of the external hazard and investigation complexity; and (4) it is recommended to use > 30 years of data and carefully interpret the extrapolation of the return period beyond four times the length of the observations.

4.2. Need for fragility analysis

The obtained results presented the necessity to examine how fragile power plants are under the condition of strong wind speeds, which are over 45 m/s. The 100-year return level of maximum wind speed and the maximum instantaneous wind speed based on the stationary model were 48.424 m/s and 58.415 m/s, respectively, which are higher than the standard wind speed level, 45 m/s, in the Shinkori safety analysis report. Moreover, the return level of instantaneous wind speed predicted by the nonstationary model with an assumption of 2034 was 82.424 m/s, which is much higher than the level indicated in the safety report. This is mainly because our study was based on the data in all domestic territories, while the results in the Shinkori report, which were estimated by Gumbel distributions, were produced only from the records in the nearest observatories. It is intuitive that the site of the Shinkori power plant, which is located on the eastern coast of the Korean Peninsula, can receive less influence from typhoons than facilities on the southwestern coast because most typhoons tend to pass the northeast of the peninsula from the southwest. However, by considering that the Korean Peninsula has an area of 223,348 km², while the radius of large

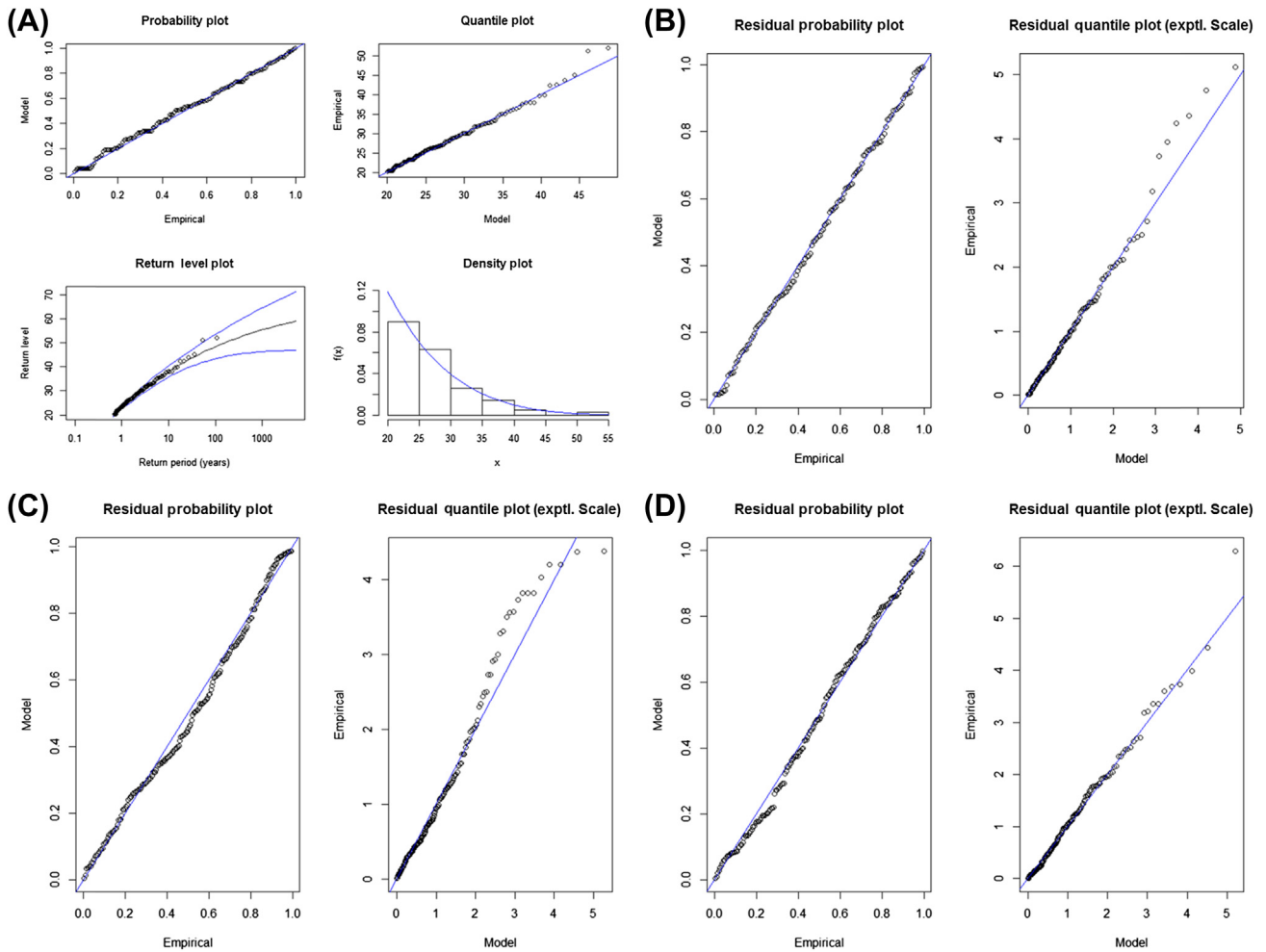


Fig. 2 – Diagnostic plots of the fitted extreme value theory model. (A) Maximum wind speed, (B) maximum instantaneous wind speed, (C) maximum hourly precipitation, and (D) maximum daily precipitation.

typhoons, i.e., the area with wind speed > 15 m/s, is > 500 km, the conservative results conducted in this study are noteworthy. Therefore, a fragility analysis of the power plants against strong wind speed will be required.

The results of the 100-year precipitation level also suggested the fragility analysis of the plants under the condition of heavy rainfall and external floods. The Shinkori safety analysis report estimated the possible maximum precipitation levels as 208 mm/h and 790 mm/d. Because the safety report considered that there are many sources that cause torrential rains aside from typhoons in Korea, the possible precipitation levels are higher than the 100-year return levels predicted by the stationary EVT models. As discussed above, since the data of this study include maximum precipitation in all domestic territories, it can be seen that both the estimated levels in the Shinkori report and this stationary model are sufficiently conservative. However, the nonstationary models, which significantly reflect the raw data more than the nested models, showed the effects of long-term climate change, and the 100-year return levels in the nonstationary models were 180.862 mm/h and 848.387 mm/d, when the input year was 2034. These values indicate the possibility of heavier rainfalls

within 100 years compared with the previously estimated levels; hence, an additional investigation would be useful to secure the safety of the facilities.

4.3. Limitations and future work

The investigations in this study were conducted based on the meteorological data related to domestic typhoons. Although the results obtained in this research are more conservative than the results based on the local observations, they can be compared with other studies based on the typhoon-related data of East Asia including Korea and neighboring countries, owing to the fact that some typhoons can simultaneously affect two countries directly or indirectly.

In this study, the 100-year return levels were frequently addressed for evaluating the hazards. Since research on probabilistic safety assessment usually deals with rare events that occur no more than once in 1,000 years, the return levels in longer return periods can be necessary for a prediction. However, as we previously discussed, the results of return periods longer than the length of the observations can have large uncertainty and confidence intervals. Therefore, a

method of robust estimation or uncertainty improvement needs to be developed for mitigating this limitation.

Heavy rainfall and strong winds can simultaneously occur in a typhoon. This study independently investigated the wind speed and rainfall, but it is also necessary to scrutinize the co-occurrence frequency of both hazards and combination effects. To analyze the co-occurrence, multivariate EVT techniques can be employed [9,13]. With reference to the combination effect, the Nuclear Energy Agency report reviewed several effects associated with extreme wind speed such as the inflow of algae into plants, water intake, loss of diesel power generators, and loss of offsite power and events related to heavy rain such as large amounts of debris intake, changes in the service water system, and loss of offsite power from landslides [3]. Knochenhauer and Louko [17] also presented the potential combinations of external events including two or more simultaneous events and introduced guidelines to analyze external events. We believe that studies on the co-occurrence frequency and combination effect based on these references will lead to a higher understanding of external hazards related to typhoons.

Conflicts of interest

All contributing authors declare no conflicts of interest.

Acknowledgments

This work was supported by the Nuclear Research and Development Program of the National Research Foundation of Korea grant, funded by the Korean government, Ministry of Science, Information and Communications Technology (ICT) and Future Planning. The authors also acknowledge the Korean meteorological administration for providing important data for this research.

REFERENCES

- [1] J.E. Yang, Development of an integrated risk assessment framework for internal/external events and all power modes, *Nuclear Engineering and Technology* 44 (2012) 459–470.
- [2] A. Mosleh, PRA: a perspective on strengths, current limitations, and possible improvements, *Nuclear Engineering and Technology* 46 (1) (2014) 1–10.
- [3] Nuclear Energy Agency Committee on the Safety of Nuclear Installations, Probabilistic Safety Analysis (PSA) of Other External Events Than Earthquake NEA/CSNI/R(2009) 4, OECD Nuclear Energy Agency, Paris, France, 2009, p. 114.
- [4] J. Sandberg, G. Thuma, G. Georgescu, Probabilistic Safety Analysis of Non-Seismic External Hazards, Radiation and Nuclear Safety Authority (STUK), Helsinki, Finland, 2009.
- [5] K.N. Fleming, On the issue of integrated risk—a PRA practitioners perspective, in: Proceedings of the ANS International Topical Meeting on Probabilistic Safety Analysis, San Francisco, 2005.
- [6] J. Vitázková, E. Cazzoli, Risk targets in view of Fukushima: facts and myths, in: Proceedings of Nordic PSA Conference – Castle Meeting, Gottröra, Sweden, 2011.
- [7] J.E. Yang, Fukushima Dai-Ichi accident: lessons learned and future actions from the risk perspectives, *Nuclear Engineering and Technology* 46 (2014) 27–38.
- [8] J. Beirlant, Y. Goegebeur, J. Segers, J. Teugels, J. Segers, *Statistics of Extremes: Theory and Applications*, John Wiley & Sons, Chichester, UK, 2004.
- [9] S. Coles, *An introduction to Statistical Modeling of Extreme Values*, Springer, London, 2001.
- [10] A.M.G. Klein Tank, F.W. Zwiers, X. Zhang, Guideline on Analysis of Extremes in a Changing Climate in Support of Informed Decisions for Adaptation, Climate Data and Monitoring. WCDMP-No. 72, WMO-TD No. 1500, Geneva, 2009.
- [11] International Atomic Energy Agency, Meteorological and Hydrological Hazards in Site Evaluation for Nuclear Installations Specific Safety Guide, Series No. SSG-18, IAEA, Vienna, 2011.
- [12] Atomic Energy Licencing Board, Guideline for Site Evaluation for Nuclear Power Plant LEM/TEK/64, 2011.
- [13] E. Gilleland, R.W. Katz, Analyzing Seasonal to Interannual Extreme Weather and Climate Variability with the Extremes Toolkit, 18th Conference on Climate Variability and Change, 86th American Meteorological Society (AMS) Annual Meeting, vol. 29, KHNP, Korea, 2006.
- [14] Y.-T. Chiu, Typhoon Haiyan: Philippines faces long road to recovery, *The Lancet* 382 (2013) 1691–1692. Elsevier, UK.
- [15] Y.T. Chiu, Typhoon Haiyan: Philippines faces long road to recovery, *The Lancet* 382 (2013) 1691–1692.
- [16] Y. Mitsuta, T. Fujii, Analysis and synthesis of typhoon wind pattern over Japan, *Bulletin of the Disaster Prevention Research Institute* 329 (1987) 169–185.
- [17] M. Knochenhauer, P. Louko, Guidance for External Events Analysis, SKI Report 02:27, 2003.